

LASERS

PACS numbers: 42.55.Px; 41.75.Fr; 42.60.Jf
DOI: 10.1070/QE2014v044n03ABEH015351

Laser radiation of CdS_xSe_{1-x} targets in a gas diode

A.S. Nasibov, K.V. Berezhnoi, M.B. Bochkarev, A.G. Sadykova, P.V. Shapkin, S.A. Shunailov

Abstract. **Laser radiation of semiconductor targets of CdS_xSe_{1-x} solid solutions excited by an electron beam in a gas-filled diode was investigated at constant and varying gas pressures. In the first case, lasing was excited by an electron beam with an energy of 170 keV and a duration of 100 ps in semiconductor targets with different x. The highest powers 125 and 96 kW were achieved at $x \approx 0.2$ ($\lambda \approx 677$ nm) and $x \approx 1$ ($\lambda \approx 522$ nm), respectively. The minimum power (26 kW) was observed in the yellow-green spectral region. The maximum slope efficiency in these experiments reached 9%. In the second case, the radiation power of CdS targets ($x = 1$) was studied as a function of the air pressure in the gas diode varying from 0.1 to 2.5 Torr. The experimental data well agree with the calculation results. The possibility of reducing the radiation divergence by using a conical optical fibre is demonstrated. At the lasing threshold of semiconductor targets exited by an electron beam or a streamer discharge, filamentary channels appear due to, probably, an anisotropy of the impact ionisation coefficient.**

Keywords: *semiconductor laser target, gas diode, electron beam.*

1. Introduction

Excitation of semiconductor lasers by an electron beam or an electric field can form high-power (10^4–10^6 W) laser pulses in the visible and UV spectral regions. Of special interest is to study the possibility of forming picosecond pulses used in medicine, in investigations of fast processes in biological tissues and in recording devices. The invention of methods for formation of ultrashort high-voltage pulses [1] created a background for further development of such lasers [2–6]. In contrast to earlier works [7, 8], a semiconductor target (ST) in our laser experiments is placed between electrodes in a gas-filled metal chamber coupled with a nanosecond pulse generator. A coaxial design of the chamber ensures a high voltage rise rate ($dU/dt > 10^{13}$ V s^{-1}). Chambers of this type are called gas diodes (GDs) and are usually used to study high-voltage nanosecond gas discharges. We study the possibility of using GDs to form picoseconds laser pulses upon excitation of STs by an electric discharge and an electron beam (EB).

A.S. Nasibov, K.V. Berezhnoi, P.V. Shapkin P.N. Lebedev Physics Institute, Russian Academy of Sciences, Leninsky prosp. 53, 119991 Moscow, Russia; e-mail: nas2121@mail.ru;
M.B. Bochkarev, A.G. Sadykova, S.A. Shunailov Institute of Electrophysics, Ural Branch, Russian Academy of Sciences, ul. Amundsena 106, 620016 Ekaterinburg, Russia

Received 25 November 2013; revision received 2 December 2013
Kvantovaya Elektronika **44** (3) 201–205 (2014)
Translated by M.N. Basieva

Among the recent results, we should mention lasing at several spectral lines obtained using semiconductor solid solutions $Cd_xZn_{1-x}S$ and CdS_xSe_{1-x} as active media [9, 10]. At the first stage of nanosecond discharge development in a GD, runaway electrons are observed even at the atmospheric gas pressure [11]. In [12], it was shown that, varying the gas (air) pressure from 0.1 to 2 Torr in a GD with a cadmium sulphide ST, one can vary the laser pulse duration from 125 to 20 ps.

In contrast to work [6], in which the spectral and dynamic characteristics of STs were measured using a high-voltage delay line, in the present work we use a fibre optic synchronisation and detection system. The main goal of our experiments was to obtain high-power picosecond laser pulses in the red-green spectral region using CdS_xSe_{1-x} solid solutions with different x as semiconductor targets. The investigations were performed at constant and variable (from 0.1 to 2.5 Torr) gas pressures.

2. Experimental

The scheme of our experimental setup with a fibre optic detection system is shown in Fig. 1. The system allows us to perform picosecond diagnostics of radiative processes in real time. The high-voltage picosecond pulse generator (VPG) operates based on sharpening the leading edge and shortening of the duration of pulses formed by a RADAN-303 generator

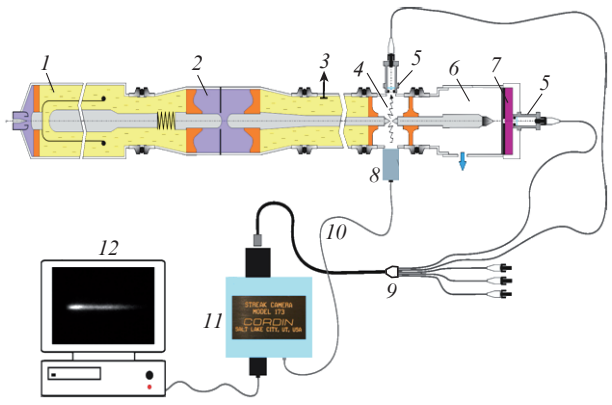

Figure 1. Schematic of the experimental setup with a fibre optic synchronisation and recording system: (*1*) RADAN-303 pulse generator; (*2*) cutting discharger (slicer); (*3*) voltage divider; (*4*) additional discharger; (*5*) focusing unit; (*6*) gas chamber; (*7*) semiconductor target; (*8*) FEK; (*9*) five-channel fibre optic system; (*10*) coaxial cable for triggering the streak camera; (*11*) streak camera; (*12*) personal computer.

(*1*) by successive switching of high-pressure (~10 atm) dischargers and a cutting ring slicer (*2*). To measure the voltage pulse parameters, a capacitive voltage divider (*3*) is inserted into the VPG transmission line. An additional discharger (*4*) serves to synchronise the VPG with recording devices. The radiation spectra and dynamics were recorded using fibre optic cables connected to the GD via connectors (*5*) with microlenses focusing radiation on the input end of the cable. After breakdown of the discharge gap of (*4*), a negative high voltage pulse (up to 200 kV) reaches an explosive emission cathode (*6*). The EB diameter on a target (*7*) is limited by an aperture (∅1 mm). The VPG is described in detail in work [5].

The SMs were made of CdS_xSe_{1-x} single-crystal films 20–30 μm thick attached to sapphire disks (*7*). The optical cavity was formed by reflective coatings ($R_1R_2 \approx 0.88$) deposited on both surfaces of the films. The dynamics and shape of the light pulse were observed using a CORDIN-173 streak camera (*11*). The streak camera was synchronised with the VPG using a FEK-22M detector (*8*). The delay time was controlled by the length of the optical cable of a five-channel system (*9*). The pulse profile was also recorded by a broadband FP-70C detector with a fibre cable with a connector (*5*) (the FP-70C response time was ~100 ps). The electron beam current was measured by a Faraday cylinder placed behind an aperture under a cathode (*6*). The laser pulse energy was measured using a J3S10 pyroelectric detector and NS attenuating filters. The radiation peak power was estimated taking into account the pulse shape. The voltage, current and radiation pulses were recorded on a Tektronix TDS-6154C oscilloscope with a band of 15 GHz. The EB duration and energy was predetermined by the slicer and then controlled by changing the air pressure in the GD chamber. The radiation spectrum was measured by a small-size FSD-8 spectrometer.

Most experiments were performed at an air pressure in the GD of 05–1 Torr. In this pressure range, the EB current amplitude was most stable. At the voltage pulse duration $t_p >$ 500 ps, on the top of the current pulse we observed two spikes whose amplitudes A_1 and A_2 depended on the pressure in the GD (Fig. 2). The oscillograms of the EB voltage and current pulses at different durations t_p and air pressures in the GD chamber are shown in Fig. 3.

The dependence of the laser wavelength on the parameter x for STs of CdS_xSe_{1-x} single crystals grown by resublimation from the gas phase [13] is shown in Fig. 4. The straight line connects the points corresponding to the wavelengths of the

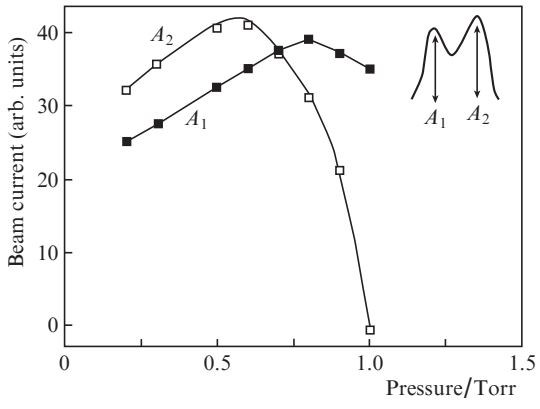

Figure 2. Dependences of the amplitudes A_1 and A_2 of the current pulse spikes on the air pressure in the GD.

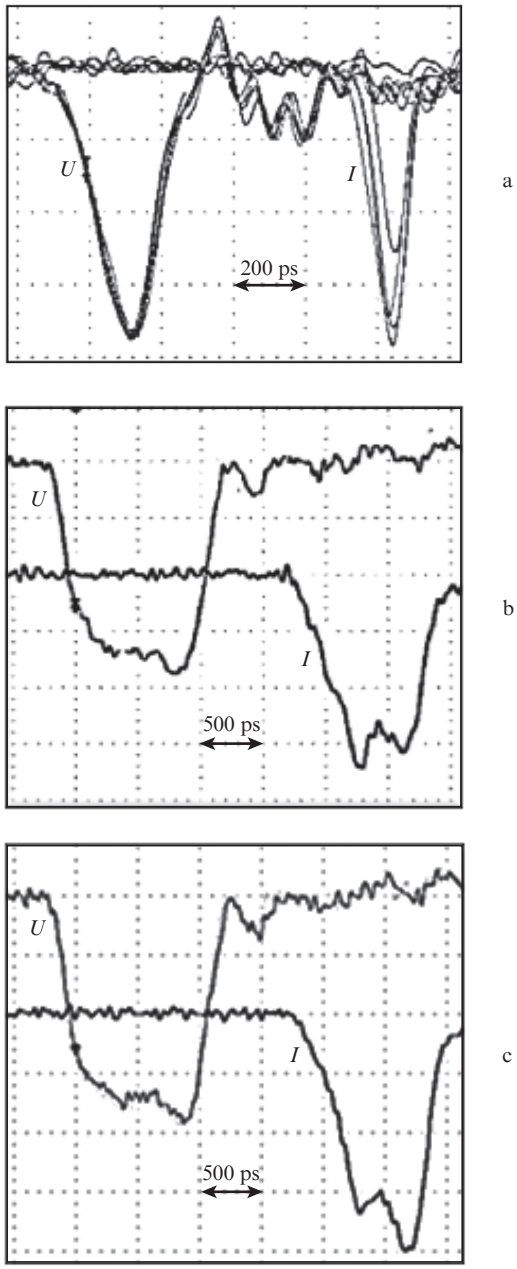

Figure 3. Oscillograms of EB voltage U and current I at U = –150 V and the following parameters: I_{max} = 4 A, p = 0.6 Torr (a); 3.5 A, 0.76 Torr (b); and 4 A, 0.58 Torr (c).

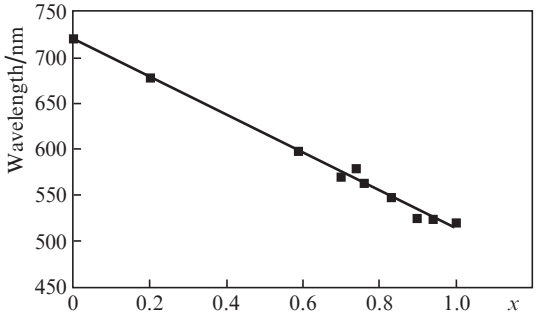

Figure 4. Dependence of the wavelength on parameter x for CdS_xSe_{1-x} single-crystal STs 30 μm thick.

CdSe (x = 0) and CdS (x = 1) binary compounds. The obtained experimental results agree with the data from the handbook on semiconductor solid solutions [14]. Altogether, we studied 12 STs with different x and obtained lasing within the range 522–677 nm, which corresponds to x changing from 1 to 0.2. The wavelength dependence of the radiation power is shown in Fig. 5. The radiation power nonmonotonically changes with variations in the target composition and noticeably decreased at x = 0.7–0.8 in the yellow-green region. The highest powers (96 and 125 kW) at a laser efficiency with respect to the absorbed pump power of 4.8% and 6% were achieved at x = 1 (x = 522 nm) and $x \approx 0.2$ (λ = 677 nm), when the ST compositions were close to the CdS or CdSe compounds. In the yellow-green spectral region, the laser efficiency decreased to 1.3%. This set of experiments was performed at a voltage of –170 kV and an EB current of 12 A. The threshold EB current density p_{th} at the pulse duration t_e = 135 ps was 8.5×10^7 W cm^{-2}, which is approximately an order of magnitude higher than 10^7 W cm^{-2} obtained in [15] at the pulse duration t_e = 4 ns under the conditions close to the conditions of our experiments.

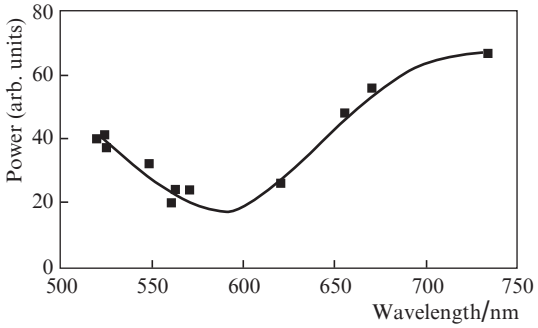

Figure 5. Wavelength dependence of the laser power for CdS_xSe_{1-x} STs.

The typical spectra of laser radiation from STs at x = 1 and 0.2 are given in Fig. 6. Figure 7 shows the dependence of the ST radiation power ($x \approx 1$, λ = 522 nm) on the air pressure in the GD. It is seen that the radiation power almost does not change while the pressure increases from 0.1 to 1 Torr and then monotonically decreases to $0.6P_{max}$ with increasing pressure. This behaviour is explained by a nonlinear dependence

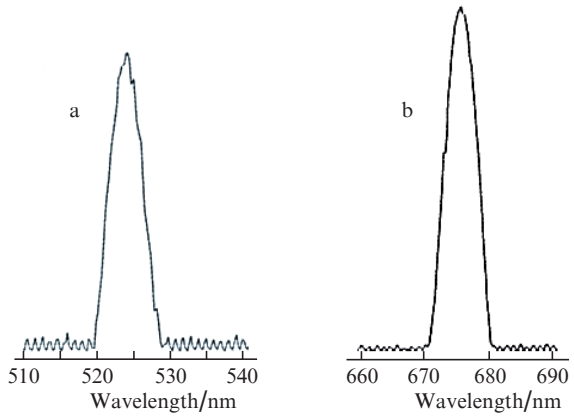

Figure 6. Lasing spectra for CdS_xSe_{1-x} STs with x = 1 (a) and 0.2 (b).

of the current pulse amplitude and duration on the gas pressure in the GD [16]. The allowance for these factors leads to good coincidence of the experimental and calculated data (Fig. 7). To excite lasing in these experiments, we used an initial voltage of –150 kW. The radiation power reached 30 and 15 kW at an electron beam pulse duration at half maximum of 125 and 80 ps, while the efficiency was ~5%. Figure 8 presents typical laser radiation pulses recorded in our experiments by the broadband FP-70C photodetector and the streak camera at different gas pressures in the GD.

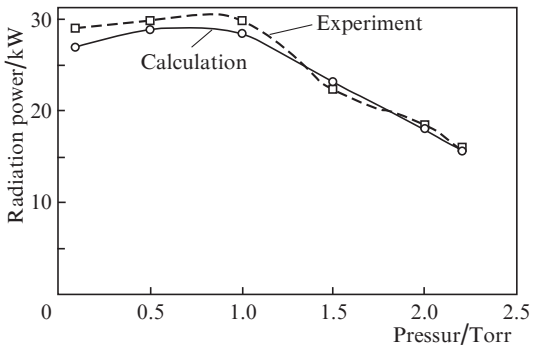

Figure 7. Dependence of the radiation power of a CdS ST on the gas pressure at U = –150 kV, t_e = 125–80 ps, and τ_0 = 1.5 ns.

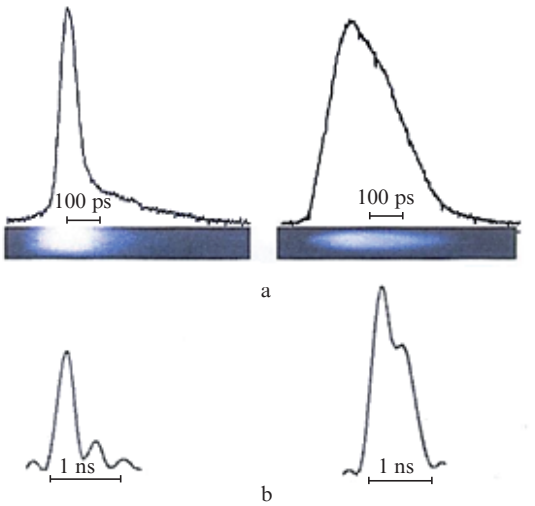

Figure 8. Laser pulses recorded by a streak camera (a) and an FP-70C photodetector (b) at different gas pressures in the GD.

The ST radiation divergence did not exceed 15°. Usually, the divergence is decreased using an external cavity [17]. In this case, the laser efficiency decreases with increasing cavity length as $1/L^2$ [15]. To decrease the divergence in our experiments, we used a conical-profile optical fibre (focon) 5 cm long with an input-to-output diameter ratio of 0.5. The input plane of the focon (with a smaller diameter) was positioned on the sapphire substrate of the SM. The near-field image on the output plane of the focon was increased in diameter by two times and the divergence angle decreased to 6–7°, while the laser efficiency remained almost unchanged.

Figure 9 shows the near-field images of radiation of a CdS_xSe_{1-x} (x = 0.2, λ = 677 nm) upon EB excitation (Figs

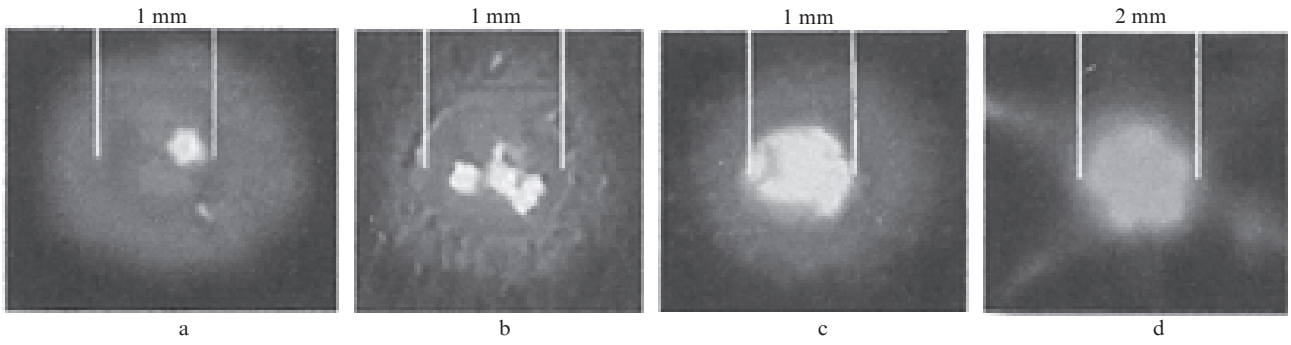

Figure 9. Near-field images of laser radiation of a CdS_xSe_{1-x} ($x \approx 0.2, \lambda = 677$ nm) ST excited by an EP with successively increasing currents (a–c) and of a CdS_xSe_{1-x} ($x \approx 0.7, \lambda = 572$ nm) target excited by a streamer discharge (d). The emitting regions consist of separate points tens of micrometers in diameter, which are poorly resolved in the photographs.

9a–9c) and of a CdS_xSe_{1-x} target ($x = 0.7, \lambda = 572$ nm) excited by a streamer discharge (Fig. 9d). The image in Fig. 9a was shot at the lasing threshold, the images in Figs 9b and 9c were obtained at an excess of the threshold, and the shot in Fig. 9d was done upon streamer-discharge excitation of a plane-parallel plate 1 mm thick with a voltage pulse amplitude of 100 kW. It is interesting that lasing in all the cases develops in separate points, whose number and diameter increase with increasing power of excitation pulses.

3. Discussion of results

To explain the observed phenomena, let us consider the basic formulas for the dependences of the laser power P_{las} on the optical cavity and electron beam parameters [7, 18, 19]

$$P_{las} = k\beta_{in} f P_p \left(1 - \frac{I_{th}}{I_p}\right), \quad (1)$$

$$f = \left[1 + \frac{2\alpha_{ex} z_{ex}}{\ln|R_1 R_2|} + \frac{2\alpha_{pas}(h - z_{ex})}{\ln|R_1 R_2|}\right]^{-1}, \quad (2)$$

$$I_{th} = I_{th0}\left[1 - \exp\left(-\frac{t_e}{\tau_0}\right)\right]^{-1}, \quad (3)$$

where $k \approx 0.1–0.2$ is the coefficient characterising energy losses for ionisation and backscattering in the case of electron beam excitation, β_{in} is the internal quantum efficiency, f is the radiation yield function, P_p is the EB pulse power, I_p is the EB current, I_{th} is the threshold EB current, I_{th0} is the threshold current at $\tau_0 \gg t_e$, τ_0 is the lifetime of nonequilibrium charge carriers, $\alpha_{ex} \approx 2–3$ cm^{-1} is the absorption coefficient in the excited ST region, $\alpha_{pas} \approx 30$ cm^{-1} is the absorption coefficient in the passive region, $z_{ex} \approx \mu_1 E_e$ is the excited region length, h is the semiconductor plate thickness, R_1 and R_2 are the reflection coefficients of the mirrors, and E_e is the EB energy. In the case of CdS ($x = 1$), $\mu_1 = 0.16$ μm keV^{-1}. As was noted above, in our case, at the EB pulse duration at half maximum $t_e = 125$ ps, the threshold EB power density is $p_{th} \approx 10^8$ W cm^{-2}. The lifetime τ_0 for CdS and CdSe at $T = 300$ K is 1–3 ns [19]. Substituting $t_e = 1.25 \times 10^{-10}$ s and $\tau_0 = 1.5 \times 10^{-9}$ s into (3), we obtain $I_{th}/I_0 \approx 12$, i.e., at a pulse duration of hundreds of picoseconds, the lasing threshold may increase by more than an order of magnitude, which well agrees with the data of [15] ($p_{th0} = 10^7$ W cm^{-2} at $t_e = 4$ ns).

Now, let us consider the wavelength dependence of the radiation power (see Fig. 5). For $\lambda = 677$ nm (CdS_xSe_{1-x}, $x \approx 0.2$) and $\lambda = 522$ nm (CdS, $x \approx 1$), we have the ratios $P_{las0.2}/P_{las1} \approx 1.3$ and $\lambda_{0.2}/\lambda_1 = 1.29$; therefore, for the ST materials closer to the CdS and CdSe binary compounds, under identical laser parameters ($h = 30$ μm, $R_1R_2 = 0.88$) and excitation by one and the same EB, the emitted power increases with increasing wavelength (with decreasing energy gap width). This dependence follows from Eqns (1) and (2).

Let us estimate the radiation power using formulas (1)–(3) with the following parameters: $k \approx 0.12$, $\beta_{in} = 1$, $h = 30$ μm, $R_1R_2 = 0.88$, $f = 0.8$, $\alpha_{ex} \approx 2.5$ cm^{-1}, $\alpha_{pas} \approx 30$ cm^{-1}, $z_{ex} = 27$ μm, $U = -170$ кВ, $P_p = 2 \times 10^6$ W, $I_{th0.2} = 4$ A, and $I_p = 12$ A. Substituting these data into (1), we obtain $P_{las} \approx 129$ kW, which well agrees with the experimental result 125 kW and points to a high quality of the close-to-binary compounds (the latter is also confirmed by the approximate equality $P_{las0.2}/P_{las1} \approx \lambda_{0.2}/\lambda_1$). The slope efficiency for the considered case is ~9%. An increase in the lasing threshold in the yellow-green region was also observed in [20], in which the authors suggested that one of the reasons for this increase is that the solid solutions obtained at high temperatures can decompose in the process of cooling into phases whose compositions are close to the binary compounds. This suggestion is indirectly confirmed by our experiments with excitation of single crystals of solid solutions by a streamer discharge, when we observed, apart from the main spectral line, the lines close to the wavelengths of binary compounds [9, 10]. In this case, one of the methods to increase the ST lasing efficiency is to decrease the film thickness to 10–15 μm. However, the fabrication of these targets runs into some technological problems.

Let us now consider the dependences of ST laser radiation power and duration on the pressure in the GD chamber. As the air pressure in the GD increases from 0.1 to ~1 Torr, the amplitudes of the current and voltage pulses change insignificantly, although their duration decreases from the trailing edge; the laser power also changes only slightly (see Fig. 7). This process relates to an increase in the GD conductivity and a decrease in the cathode–target gap breakdown time. With increasing gas pressure, the gap breakdown occurs on the leading edge of the voltage pulse and, hence, the amplitudes and durations of the voltage and current pulses decrease (in our case, the current pulse duration at half maximum changed from 125 to 80 ps). The decrease in the exciting EB current and duration with changing the pressure from 1 to 2.5 Torr leads to a decrease in the radiation duration and power (from 30 to 15 kW). The dependences of the radiation power on the air pressure in the GD calculated taking into account the change in the exciting EB power and the dependence of the

lasing threshold on the pulse duration (3) well coincide with experimental data (Fig. 7).

It is interesting to look at the near-filed images of CdSSe laser radiation in the case of excitation by an EB and a streamer discharge (Fig. 9). The appearance of lasing channels in the form of bright points with diameters from a few to hundreds of micrometers, in which the conditions are favourable for lasing onset, was observed long ago [21] but has not been clearly explained until now. The similarity of the images in the case of EB and discharge excitation allows one to suggest that the reason for the appearance of points is an anisotropy of impact ionisation coefficients, which leads to the formation of channels and propagation of a streamer in a particular crystallographic direction [22, 23].

Thus, we have demonstrated the possibility of obtaining laser radiation from semiconductor targets of a gas diode with pressures from 0.1 to 2.5 Torr in the visible spectral region (500–700 nm) with a duration from 1 ns to 100 ps and a power of tens–hundreds of kilowatts. The decrease in the laser efficiency in the yellow-green region is obviously related to an inhomogeneity of solid solutions and can be compensated by optimising the cavity parameters and improving the quality of the crystals.

Acknowledgements. This work was supported by the Russian Foundation for Basic Research (Grant No. 12-08-00263-a).

References

1. Mesyatz G.A., Yalandin M.I. *Usp. Fiz. Nauk*, **175** (3), 225 (2005).
2. Mesyatz G.A., Nasibov A.S., Shpak V.G., Shunailov S.A., Yalandin M.I. *Zh. Eksp. Teor. Fiz*., **133** (6), 1162 (2008).
3. Mesyats G.A., Nasibov A.S., Shpak V.G., Shunailov S.A., Yalandin M.I. *Kvantovaya Elektron*., **38** (3), 213 (2008) [*Quantum Electron*., **38** (3), 213 (2008)].
4. Berezhnoi K.A., Nasibov A.S., Shapkin P.V., Shpak V.G., Shunailov S.A., Yalandin M.I. *Kvantovaya Elektron*., **38** (9), 829 (2008) [*Quantum Electron*., **38** (9), 829 (2008)].
5. Nasibov A.S., Berezhnoi K.V., Shapkin P.V., Reutova A.G., Shunailov S.A., Yalandin M.I. *Prib. Tekh. Eksp*., **1**, 75 (2009).
6. Berezhnoi K.V., Bochkarev M.B., Nasibov A.S., Reutova A.G., Shunailov S.A., Yalandin M.I. *Prib. Tekh. Eksp*., **2**, 124 (2010).
7. Bogdankevich O.V., Darznek S.A., Eliseev P.G. *Poluprovodnikovye lazery* (Semiconductor Lasers) (Moscow: Nauka, 1976).
8. Kryukova I.V. *Fizicheskie prozessy v poluprovodnikovykh impul'snukh lazerakh s nakachkoi elektronnymi puchkami* (Physical Processes in Pulsed Semiconductor Lasers Pumped by Electron Beams) (Moscow: Bauman MSTU Press, 2009).
9. Nasibov A.S., Danielyan G.D., Bagramov V.G., Berezhnoi K.V. *Kratk. Soobshch. Fiz. FIAN*, (4), 17 (2011).
10. Nasibov A.S., Bagramov V.G., Berezhnoi K.V., Shapkin P.V. *Kratk. Soobshch. Fiz. FIAN*, (4), 25 (2013).
11. Tarasenko V.F., Shpak V.G., Shunailov S.A., Yalandin M.P., Orlovskii V.M., Alekseev S.V. *Pis'ma Zh. Teor. Fiz*., **29** (21), 1 (2003).
12. Berezhnoi K.V., Bochkarev M.B., Danielyan G.L., Nasibov A.S., Reutova A.G., Shunailov S.A., Yalandin M.I. *Kvantovaya Elektron*., **42** (1), 34 (2012) [*Quantum Electron*., **42** (1), 34 (2012)].
13. Korostelin Yu.V., Kozlovsky V.I., Nasibov A.S., Shapkin P.V. *J. Cryst. Growth*, **161**, 51 (1996).
14. Berchenko N.I., Krevs V.E., Sredin V.G. *Poluprovodnikovye tverdye rastvory i ikh primenenie* (Semiconductor Solid Solutions and Their Application) (Moscow: Voenizdat, 1982).
15. Daneu V., DeGloria D.P., Sanchez A., Osgood R.M. *Appl. Phys. Lett*., **49** (10), 8 (1986).
16. Nasibov A.S., Berezhnoi K.V., Bochkarev M.B., Danielyan G.L., Reutova A.G., Shunailov S.A. *Dokl. 20th Mezhd. konf. 'Lazery, izmereniya, informatsiya'* (Proc. 20th Int. Conf. 'Lasers, Measurements, Information') (St. Petersburg: GPU Press, 2010) Vol. 1, p. 5.
17. Basov N.G., Bogdankevich O.V., Pechenov A.N., Nasibov A.S., Fedoseev K.P. *Zh. Eksp. Teor. Fiz*., **55**, 1710 (1969).
18. Bogdankevich O.V., Zverev M.M., Krasavina E.M., et al. *Kvantovaya Elektron*., **14** (1), 218 (1987) [*Sov. J. Quantum Electron*., **17** (1), 133 (1987)].
19. Kozlovskii V.I., Popov Yu.M. *Kvantovaya Elektron*., **33** (1), 48 (2003) [*Quantum Electron*., **33** (1), 48 (2003)].
20. Akhekyan A.M., Kozlovskii V.I., Korostelin Yu.V., Reznikov P.V., Tikhonov V.G., Shapkin P.V. *Trudy FIAN*, **202**, 128 (1991).
21. Kozlovskii V.I., Nasibov A.S., Pechenov A.N. *Kvantovaya Elektron*., **4** (2), 351 (1977) [*Sov. J. Quantum Electron*., **7** (2), 194 (1977)].
22. Basov N.G., Molchanov A.G., Nasibov A.S., Obidin A.Z., Pechenov A.N., Popov Yu.M. *Zh. Eksp. Teor. Fiz*., **70** (5), 1751 (1976).
23. Obidin A.Z., Pechenov A.N., Popov Yu.M., Frolov V.A., Nasibov A.S. *Kvantovaya Elektron*., **9** (8), 1530 (1982) [*Sov. J. Quantum Electron*., **12** (8), 980 (1982)].